Journal of Materials Chemistry C

PAPER

View Article Online
View Journal

Cite this: DOI: 10.1039/c4tc02126f

Reversible mechanochromic luminescence of phenothiazine-based 10,10′-bianthracene derivatives with different lengths of alkyl chains†

Pengchong Xue,*[a] Boqi Yao,[a] Xuhui Liu,[b] Jiabao Sun,[a] Peng Gong,[a] Zhenqi Zhang,[a] Chong Qian,[a] Yuan Zhang[c] and Ran Lu*[a]

Received 21st September 2014
Accepted 20th November 2014

DOI: 10.1039/c4tc02126f

www.rsc.org/MaterialsC

A series of 10,10′-bis(2-(*N*-alkylphenothiazine-3-yl)vinyl)-9,9′-bianthracene compounds (**PVBAn**, $n = 2$, 8, 12 and 16) with different lengths of *N*-alkyl chains have been designed and synthesized to systematically investigate the effect of chain length on their solid-state fluorescence properties. The results showed that these compounds emitted strong fluorescence in solution and in the solid state. Their emission wavelengths were also strongly affected by solvent polarity, indicating intramolecular charge transfer (ICT) transitions. Interestingly, the fluorescence emission and grinding-induced spectral shifts of **PVBAn** solids are alkyl length-dependent. **PVBA2** shows the smallest fluorescence and absorption spectrum shifts under mechanical force stimuli. Homologues with longer alkyl chains exhibit similar mechanochromic behaviors and larger fluorescence contrasts after grinding. Moreover, the fluorescence emission of ground solid **PVBA16** can recover at room temperature, but other compounds need high temperatures for fluorescence to be restored. Differential scanning calorimetry experiments reveal that the cold-crystallization temperature difference is responsible for thermal restoration behaviors. This work demonstrates the feasibility of tuning the solid-state optical properties of fluorescent organic compounds by combining the simple alteration of chemical structure and the physical change of aggregate morphology under external stimuli.

Introduction

Conjugated organic molecules exhibiting solid-state fluorescence are promising optical and optoelectronic materials and are applied in organic light-emitting diodes, lasers, and sensors. Among them, some fluorescent organic molecules exhibit tunable and switching solid-state luminescence by external mechanical stimuli, which is known as mechanofluorochromism (MFC).[1] As a kind of "smart material,"[2] MFC compounds have attracted significant attention because of their promising applications in optical storage, pressure sensors, rewritable media, and security ink.[3] These fluorescent organic molecules can show changes in the color of their fluorescence under mechanical stress and be restored to their original state by annealing or fuming with solvent vapor.[4] Generally, no chemical structure damage occurs during the reversible emissive color change process, and only the molecular packing model in the solid state is changed under a pressure stimulus.[5] However, MFC materials are still at the initial stages of investigation, and the types of MFC materials and in-depth understanding of MFC phenomena are limited. Moreover, the identification of most MFC compound is still an isolated event. Therefore, there is still a great demand for identifying new MFC materials, as well as the accumulation of knowledge of the relationships between molecular structure and properties. To date, many kinds of organic molecules have been exploited to produce MFC properties. For example, Araki *et al.* and Kato *et al.* found that some hydrogen-bonded self-assemblies and liquid crystals could exhibit responses to force stimuli.[6] Harima designed a series of heteropolycyclic fluorescent dyes, which have MFC behaviors, and suggested that D–π–A emissive molecules always contribute to the realization of fluorescence change under pressure.[7] More importantly, nonplanar π-conjugated emissive molecules, such as tetraphenylethene, 9,10-divinylanthracene, triphenylamine derivatives and organoboron compounds, are preferentially considered to act as MFC materials.[8] Phenothiazine is an excellent functional block

[a]*State Key Laboratory of Supramolecular Structure and Materials, College of Chemistry, Jilin University, No. 2699 Qianjin Street, Changchun, P. R. China. E-mail: xuepengchong@jlu.edu.cn; luran@mail.jlu.edu.cn*

[b]*Taiyuan Center for Disease Control and Prevention, No. 89 Xinjiannan Road, Taiyuan, P. R. China*

[c]*College of Chemistry, Beijing Normal University, No. 19, Xinjiekouwai Street, Haidian District, Beijing, China*

† Electronic supplementary information (ESI) available: NMR and MS spectra; plot of emission maximum energy *vs.* solvent polarity; absorption and emission spectra in different solvents; stimulated absorption spectra and electron transition data; frontier orbitals; IR, UV-vis, fluorescence and time-resolved fluorescence spectra of solids; tables about photophysical data and recovery times at different temperatures. See DOI: 10.1039/c4tc02126f

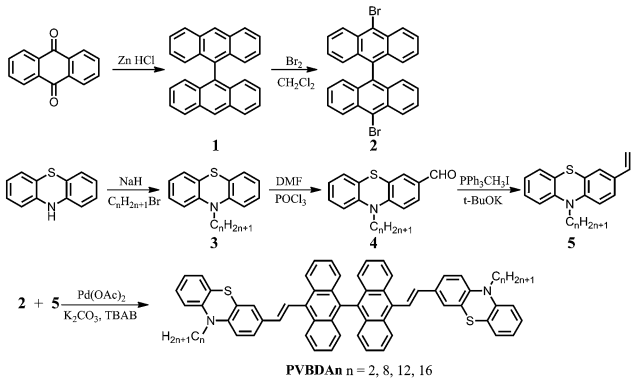

Scheme 1 Synthesis route for obtaining **PVBAn**.

for the construction of organic luminescent materials.[9] It has a nonplanar, bowl-shaped configuration, and recently it has been introduced into molecular structures to obtain MFC-active fluorescent molecules.[10] Moreover, 9,9′-bianthracene has a twisted conformation due to the strong repulsive interaction of the hydrogen atoms at the 1,1′ and 8,8′ positions.[11] It is expected that the molecular material will have excellent MFC properties if nonplanar phenothiazine and 9,9′-bianthracene are integrated in one molecule.

Moreover, slight differences in molecular structure will induce distinct emissive behaviors. For instance, changing the length of the *n*-alkyl chain can effectively adjust the MFC behavior and thermodynamic properties.[12] In this study, we have designed and facilely synthesized a series of 10,10′-bis(2-(*N*-alkylphenothiazine-3-yl)vinyl)-9,9′-bianthracenes with ethyl, octyl, dodecyl and hexadecyl as alkyl side chains (**PVBAn**, Scheme 1), and their fluorescence properties and MFC behavior were investigated. The results show that these molecules indeed exhibit MFC activity and their fluorescence emission and MFC behaviors are alkyl length-dependent. **PVBA16** showed an isothermally reversible fluorescence switching of an MFC material because of its spontaneous restoration at room temperature.

Experimental section

General information

All the raw materials were used without further purification. All the solvents were of analytical reagent grade and purchased from Beijing Chemical Works (Beijing, China); moreover, they were used without further purification. The water used in all the experiments was purified with a Millipore system. The UV-vis absorption spectra were obtained using a VARIAN Cary 50 Probe spectrophotometer. The absorption spectra of solids were obtained by measuring their films on the surface of a silica plate. Photoluminescence measurements were obtained on a Cary Eclipse fluorescence spectrophotometer. The fluorescence quantum yields of **PVBAn** (n = 2, 8, 12 and 16) in various solvents were measured by comparing with a standard (9,10-diphenyl anthracene in benzene, Φ_F = 0.85). Note that the excitation wavelength was 410 nm. Mass spectra were obtained with AXIMA CFR MALDI-TOF (Compact) mass spectrometers. C, H, and N elemental analyses were performed with a PerkinElmer 240C elemental analyzer. The XRD patterns were obtained on an Empyrean X-ray diffraction instrument equipped with graphite-monochromatized Cu Kα radiation (λ = 1.5418 Å) by employing a scanning rate of 0.026° s^{-1} in the 2θ range from 5° to 30°. The samples were prepared by casting crystal powders, ground solids and fuming samples on silicon slides at room temperature. Differential scanning calorimetry (DSC) curves were obtained on a Netzsch DSC 204F1 at a heating rate of 10 °C min^{-1}. The data of all samples (pristine and ground) were collected when they were heated for the first time. Cold-crystallization of ground solids was employed using a temperature-controlled heating board. Ground powders on a weighted paper were first placed on a heating board with a measured temperature, covered by a glass plate, and then timed for emissive color recovery. The fluorescence decay experiment was measured on an Edinburgh FLS920 steady state fluorimeter equipped with an nF900 nanosecond flash lamp. The molecular configuration was used to obtain the frontier orbitals of **PVBAn** by density functional theory (DFT) calculations at the B3LYP/6-31G(d,P) level with the Gaussian 09W program package.

Synthesis, procedures, and characterization

Compounds **1**, **2**, **3**, **4**, and **5** were synthesized by the reported methods.[13] **PVBAn** were easily obtained by a one-step Heck cross-coupling reaction using 10,10′-dibromo-9,9′-bianthracene and the corresponding *N*-alkyl-3-vinyl-phenothiazine, as shown in Scheme 1.

10,10′-Bis((*E*)-2-(10-ethyl-10*H*-phenothiazine-3-yl)vinyl)-9,9′-bianthracene (PVBA2). Anhydrous K_2CO_3 (0.55 g, 4.0 mmol) and $Pd(OAc)_2$ (2.5 mg) were added to a solution of 10,10′-dibromo-9,9′-bianthracene (0.50 g, 0.98 mmol), 10-ethyl-3-vinyl-10*H*-phenothiazine (0.50 g, 1.96 mmol) and Bu_4NBr (1.3 g, 4 mmol) in dry DMF (20 mL). The mixture was stirred at 110 °C under a N_2 atmosphere for 18 h. After cooling to room temperature, the mixture was poured into water (200 mL) and extracted with CH_2Cl_2. The combined organic phases were washed with brine, and dried with anhydrous Na_2SO_4. After the solvent was removed, the residue was purified by column chromatography (silica gel, petroleum ether/methylene chloride = 4 : 1, v/v) to give 0.59 g of an orange-colored solid (70% in yield). Element analysis (%): calculated for $C_{60}H_{44}N_2S_2$: C, 84.08; H, 5.17; N, 3.27; found: C, 84.03; H, 5.13; N, 3.31; ^{1}H NMR (400 MHz, $CDCl_3$) δ 8.53 (d, J = 8.9 Hz, 4H), 7.99 (d, J = 16.5 Hz, 2H), 7.61 (d, J = 1.7 Hz, 2H), 7.52 (dd, J = 8.3, 1.5 Hz, 2H), 7.46 (m, 4H), 7.26–7.14 (m, 12H), 7.08–6.96 (m, 8H), 4.04 (q, J = 6.8 Hz, 4H), 1.53 (t, J = 6.9 Hz, 6H) (Fig. S1†). ^{13}C NMR (101 MHz, $CDCl_3$) δ 144.57, 136.46, 133.71, 133.13, 132.01, 131.52, 129.66, 127.48, 127.41, 126.39, 126.14, 125.65, 125.36, 124.99, 123.89, 123.43, 122.65, 115.31, 115.26, 53.45, 42.17, 13.04 (Fig. S2†). MALDI-TOF MS (m/z): calcd. for $C_{60}H_{44}N_2S_2$: 856.3; found: 857.4 $[M + H]^+$ (Fig. S3†).

Other 10,10′-bis(2-(*N*-alkylphenothiazine-3-yl)vinyl)-9,9′-bianthracenes were synthesized as per the same procedure that

was followed for **PVBA2**, except that different *N*-alkyl-3-vinyl-10*H*-phenothiazines were used.

10,10′-Bis((*E*)-2-(10-octyl-10*H*-phenothiazine-3-yl)vinyl)-9,9′-bianthracene (PVBA8). This compound was obtained as a yellow solid with 82% yield. Element analysis (%): calculated for $C_{72}H_{68}N_2S_2$: C, 84.33; H, 6.68; N, 2.73; found: C, 84.29; H, 6.70; N, 2.69. ^{1}H NMR (400 MHz, $CDCl_3$) δ 8.53 (d, J = 8.8 Hz, 4H), 7.98 (d, J = 16.6 Hz, 2H), 7.61 (s, 2H), 7.52 (d, J = 8.3 Hz, 2H), 7.49–7.40 (m, 4H), 7.26–7.13 (m, 12H), 7.07–6.93 (m, 8H), 3.95 (s, 4H), 1.91 (m, 4H), 1.52 (m, 4H), 1.35 (m, 16H), 0.92 (t, J = 6.2 Hz, 6H) (Fig. S4†). ^{13}C NMR (101 MHz, $CDCl_3$) δ 144.90, 136.49, 133.72, 133.13, 132.04, 131.52, 129.67, 127.54, 127.40, 127.38, 126.39, 126.09, 125.65, 125.36, 125.06, 124.39, 123.43, 122.67, 115.65, 115.58, 47.79, 31.81, 29.28, 27.00, 22.69, 14.16 (Fig. S5†). MALDI-TOF MS (*m*/*z*): calcd. for $C_{72}H_{68}N_2S_2$: 1024.5; found: 1025.3 $(M + H)^+$ (Fig. S6†).

10,10′-Bis((*E*)-2-(10-dodecyl-10*H*-phenothiazine-3-yl)vinyl)-9,9′-bianthracene (PVBA12). The compound was obtained as a yellow solid with 79% yield. Element analysis (%): calculated for $C_{80}H_{84}N_2S_2$: C, 84.46; H, 7.44; N, 2.46; found: C, 84.43; H, 7.49; N, 2.45. ^{1}H NMR (400 MHz, $CDCl_3$) δ 8.52 (d, J = 8.9 Hz, 4H), 7.98 (d, J = 16.3 Hz, 2H), 7.61 (s, 2H), 7.52 (d, J = 8.3 Hz, 2H), 7.49–7.42 (m, 4H), 7.26–7.13 (m, 12H), 7.10–6.93 (m, 8H), 3.95 (s, 4H), 1.97–1.85 (m, 4H), 1.56–1.47 (m, 4H), 1.45–1.24 (m, 32H), 0.91 (t, J = 6.8 Hz, 6H) (Fig. S7†). ^{13}C NMR (101 MHz, $CDCl_3$) δ 144.80, 136.47, 133.69, 133.13, 132.00, 131.51, 129.67, 127.49, 127.40, 127.37, 126.38, 126.08, 125.63, 125.35, 125.02, 123.92, 123.45, 122.70, 115.67, 115.61, 47.73, 31.95, 29.68, 29.62, 29.59, 29.38, 29.33, 27.00, 22.73, 14.16 (Fig. S8†). MALDI-TOF MS (*m*/*z*): calcd. for $C_{80}H_{84}N_2S_2$: 1136.6; found: 1137.5 $(M + H)^+$ (Fig. S9†).

10,10′-Bis((*E*)-2-(10-hexadecyl-10*H*-phenothiazine-3-yl)vinyl)-9,9′-bianthracene (PVBA16). The compound was obtained as a yellow solid with 85% yield. Element analysis (%): calculated for $C_{88}H_{100}N_2S_2$; C, 84.56; H, 8.06; N, 2.24; found: C, 84.51; H, 8.10; N, 2.22. ^{1}H NMR (400 MHz, $CDCl_3$) δ 8.53 (d, J = 8.9 Hz, 4H), 7.98 (d, J = 16.4 Hz, 2H), 7.61 (s, 2H), 7.52 (d, J = 7.9 Hz, 2H), 7.49–7.42 (m, 4H), 7.27–7.14 (m, 12H), 7.09–6.93 (m, 8H), 3.95 (s, 4H), 1.98–1.85 (m, 4H), 1.51 (m, 4H), 1.45–1.22 (m, 48H), 0.91 (t, J = 6.4 Hz, 6H) (Fig. S10†). ^{13}C NMR (101 MHz, $CDCl_3$) δ 144.97, 136.50, 133.73, 133.13, 131.99, 131.53, 129.67, 127.54, 127.40, 127.37, 126.40, 126.09, 125.65, 125.35, 125.07, 124.38, 123.39, 122.64, 115.60, 115.54, 47.75, 31.96, 29.75, 29.71, 29.63, 29.61, 29.40, 29.34, 27.02, 22.73, 14.17 (Fig. S11†). MALDI-TOF MS (*m*/*z*): calcd. for $C_{88}H_{100}N_2S_2$: 1248.7; found: 1249.9 $(M + H)^+$ (Fig. S12†).

Results and discussion

Photophysical properties in solution

Recent studies have demonstrated that a D–π–A–π–D fluorescent dye molecule with a large dipole is a good choice for developing MFC dyes.[14] Thus, we initially studied their spectral characteristics in solution to understand their donor–acceptor–donor π-conjugated systems. Because all the compounds have the same chromophore, **PVBA8** is used as a sample. As shown in Fig. 1, **PVBA8** has an absorption band with a maximum of 416 nm in nonpolar *n*-hexane and cyclohexane, which red-shifted to 422 nm in THF and CH_2Cl_2, to 421 nm in acetone, and to 426 nm in DMF. The red-shift of the absorption peak in polar solvents suggests that **PVBA8** is a polar molecule,[15] which can be confirmed by quantum chemical calculations.

Quantum chemical calculations were performed by density functional theory calculations at the B3LYP/6-31G(d,p) level. The calculated dipole moment is 3.03 D. Moreover, we found that the fluorescence of **PVBA8** also exhibits solvatochromism. As shown in Fig. 1b and c, **PVBA8** emits strong green fluorescence (fluorescence quantum yield, $\Phi_F = 0.4$) in hexane, and the maximal emission peak is located at 524 nm. In cyclohexane, the emission band slightly shifts to 530 nm, whereas the toluene solution has strong yellow emission ($\Phi_F = 0.33$, λ_{em} = 558 nm). Further increase in solvent polarity leads to continuous red-shift in fluorescence spectra. Note that the acetone solution has weak red fluorescence. The emission maximum reaches 658 nm in DMF with larger polarity, but Φ_F is only 0.02. In addition, Fig. 2b shows that polar solvents induce wide emission bands. The large shift of the emission band, the decrease of Φ_F, and the broadening of the emission bands in polar solvents indicate an intramolecular charge-transfer (ICT) characteristic for the excited state.[16] Lippert–Mataga plots also confirms the ICT transition because a linear relationship between maximum emission energy and solvent polarity is observed (Fig. S13†). For the other three compounds, similar spectral behaviors were found because they have the same

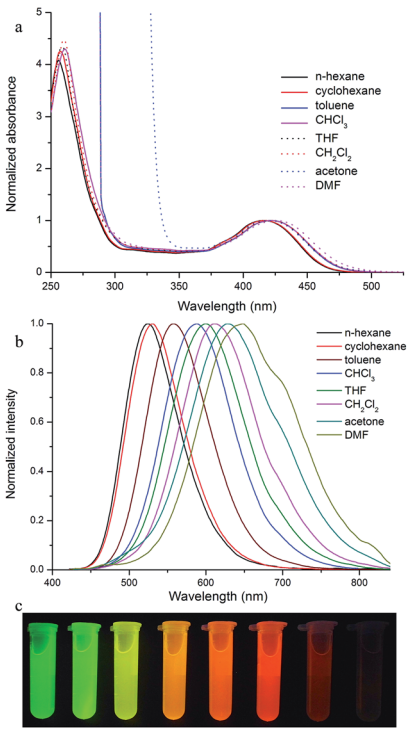

Fig. 1 Normalized solvent-dependent (a) UV-vis absorption and (b) fluorescence spectra of PVBA8. The concentration of the samples was 10^{-5} M. (c) Photos of solutions upon 365 nm light irradiation. The concentration of all samples was 10^{-5} M. λ_{ex} = 400 nm.

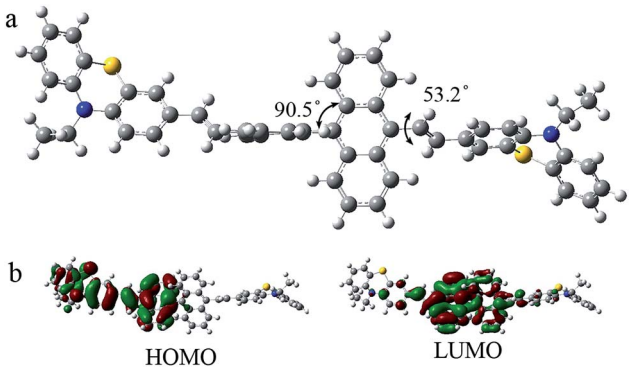

Fig. 2 (a) Optimized molecular structure and (b) electron density distributions of the frontier molecular orbitals of **PVBA2**.

chromophore (Fig. S14†). The detailed data are listed in Table S1 and S2.†

Considering the molecular structure, **PVBAn** are typical D–π–A–π–D molecules, in which bianthracene acts as an electron-withdrawing group, two phenothiazine groups are electron donors and vinyl moieties play the role of π-bridge units. Quantum chemical calculations also confirmed this conclusion. After geometry optimization (Fig. 2a), the absorption spectrum was simulated by the time-dependent DFT calculation at the B3LYP/6-31G(d,p) level. A wide absorption band with a maximum at 453.84 nm was found (Fig. S15†), which consists of one strong and two weak absorption bands. The detailed results are listed in Table S3.† The results show that electron transitions corresponding to absorption bands involve six frontier orbitals (Fig. 2b and S16†) and each transition will induce charge transfer from phenothiazine to anthracene, which results in an excited state with a larger polarity relative to that of the ground state. Furthermore, the twisted angles of the two anthracenes and between anthracene and the vinyl moiety reach 90.5° and 53.2°, suggesting a nonplanar molecular conformation. Therefore, **PVBAn** are polar and nonplanar molecules and mechanochromic activity is expected for them in the solid state.[17]

MFC properties of PVBAn

First, the spectral properties of the pristine solids were studied. It was found that the color and fluorescence color of the pristine solids are relative to the length of the alkyl chains. **PVBA2** appended with two ethyl groups at the phenothiazine units is an orange solid, but other compounds with longer alkyl chains have a yellow color. Their absorption spectra can explain the difference in color. As shown in Fig. 3a, an absorption peak at 453 nm for **PVBA2** appears, and other compounds have similar absorption maxima around 422 nm (Table 1). The absorption band at 453 nm for **PVBA2** explains its orange color. It should be noted that the absorption peaks of the solids, except for **PVBA2**, are similar to those in *n*-hexane, which indicates very weak or no π–π interaction between aromatic moieties of **PVBAn** with longer alkyl chains. In contrast, a π–π interaction exists in solid **PVBA2**, and the molecules pack together to form J-aggregates

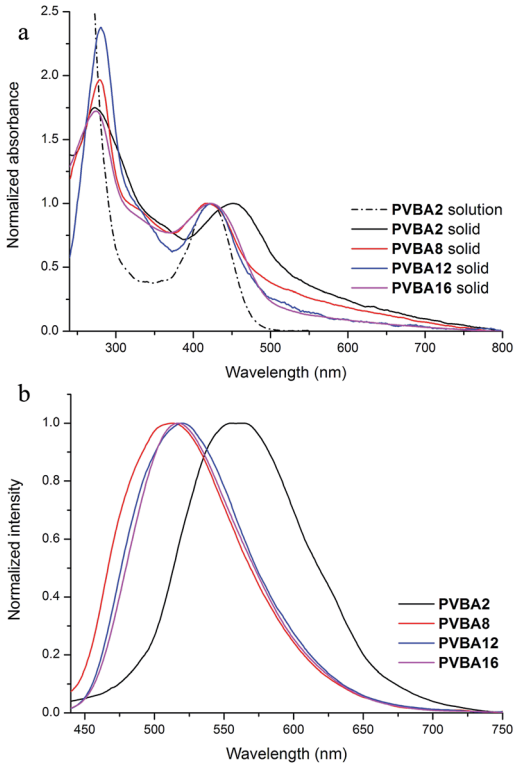

Fig. 3 (a) Absorption and (b) fluorescence of pristine **PVBAn** solid. $\lambda_{ex} = 400$ nm.

because of a red-shift in absorption.[18] The asymmetric and symmetric CH_2 stretching vibrations in the FT-IR spectra of **PVBA8–16** are located at 2917 and 2850 cm^{-1} (Fig. S17†), respectively, indicating that long alkyl chains adopt a *trans*-conformation in the solid state.[19] Thus, the longer alkyl chains will prevent aromatic units from being close to one another. In contrast, ethyl groups with short lengths will allow a significant π–π stacking; therefore, the length of the alkyl chain is responsible for the differences in color. Although X-ray analysis of single crystals could give more accurate information in molecular packing, high-quality single crystals of **PVBAn** were not obtained. Moreover, **PVBA2** has a difference in emission color as compared to the other compounds. As shown in Fig. 3b, the maximum emission peak of **PVBA2** in pristine solid state is located at 560 nm, allowing it to have yellow fluorescence with light irradiated at 365 nm. Other compounds have similar

Table 1 The data of absorption and emission peaks and lifetimes before and after grinding

	λ_{abs} (nm)		λ_{em} (nm)		τ (ns)	
	Pristine	Ground	Pristine	Ground	Pristine	Ground
PVBA2	453	433	560	580	2.5	3.4
PVBA8	418	433	513	568	1.9	3.0
PVBA12	422.5	433	519	563	—	—
PVBA16	422.5	441	517	559	—	—

emissions with a maxima around 515 nm, indicating green fluorescence. The red-shifted emission for **PVBA2** is ascribed to π–π interaction; thus, different MFC behaviors are expected for the different **PVBAn**.

When the pristine solids were ground with a spatula, orange **PVBA2** changed into orange-red powder, and other yellow solids converted into orange powders. The UV-vis spectra before and after grinding were compared (Fig. S18†). The absorption peak of the **PVBA2** pristine solid at 453 nm shifts to 443 nm after grinding, which is still red-shifted relative to that in *n*-hexane. This result shows that **PVBA2** still retained J-aggregate properties in the ground state; however, π–π interaction is weaker than that in the pristine solid after grinding. Grinding induces a red-shift of the absorption band of **PVBA8** from 417 nm to 443 nm. Other compounds show a spectral shift similar to that of **PVBA8**, and all of ground powders have almost the same absorption bands (Fig. S18e†). Such spectral changes clearly indicate that all the compounds have similar π–π interactions and form J-aggregates after grinding, independent of the length of alkyl chains. In other words, mechanical force results in the disappearance of the steric effect of the long alkyl chains and promotes similar J-aggregation between aromatic units.

As discussed above, mechanical force stimulus leading to color change, or MFC, is expected for all of the compounds. As shown in Fig. 4, the fluorescence spectra of the pristine **PVBAn** powders shift to longer wavelengths. The ground powders, except for **PVBA2**, had similar emission bands and yellow fluorescence (Fig. S19†). **PVBA2** emitted orange fluorescence with a maximum at 580 nm after grinding. The reason why **PVBA2** emits orange fluorescence is because of the existence of aggregates with low energy levels, which act as energy acceptors that quench fluorescence of short emission wavelength.[20] Time-resolved fluorescence spectra were measured to verify this. Note that the fluorescence average lifetime ($\langle\tau\rangle$) of the pristine **PVBA2** solid is 2.5 ns, which increases to 3.4 ns after grinding (Fig. S20†). The increase in lifetime could be ascribed to energy transfer because the energy acceptors with longer emission wavelengths achieve extra lifetime from donors. Grinding also caused an increase in the lifetimes of the other compounds with longer alkyl chains. For example, the ground **PVBA8** powder possesses a longer lifetime ($\langle\tau\rangle$ = 3.0 ns) relative to that of the pristine one ($\langle\tau\rangle$ = 1.9 ns). The increased π–π interaction and energy transfer should be responsible for the increase in τ.[21]

When the ground powders were exposed to organic vapors, such as those of CH_2Cl_2, $CHCl_3$, THF, toluene, hexane, cyclohexane and petroleum ether, for several seconds, the color rapidly changed into a new one (Fig. S18†). For example, after fuming, the color of the ground **PVBA8** changed from orange to yellow; moreover, fuming also caused a recovery in fluorescence (Fig. 4). These color change processes for the four compounds can be repeated many times, indicating reversible MFC behavior.[22] Therefore, **PVBAn** exhibits piezochromic behavior, not only in the fluorescence spectra, but also in the absorption spectra.

To gain an insight into the MFC behavior of **PVBAn** solids, powder wide-angle X-ray diffraction experiments were conducted on the pristine, ground and fuming solids. As shown in Fig. 5, the pristine solids show sharp and intense reflections, indicative of the well-ordered microcrystalline structures. In contrast, the ground solids display broad and weak peaks, indicating that the ground powders were amorphous.[23] After fuming by CH_2Cl_2 vapor, sharp and strong diffraction peaks similar to those of the pristine solids appeared again, suggesting the regeneration of the microcrystalline structures. Therefore, the phase transition of **PVBAn** solids between crystalline and amorphous states could be responsible for their MFC behavior. Because the crystalline state is more stable than the amorphous one, an increase in the mobility of molecules induced by solvent fuming will promote molecular rearrangement from a metastable amorphous structure to a more stable crystalline state.[24]

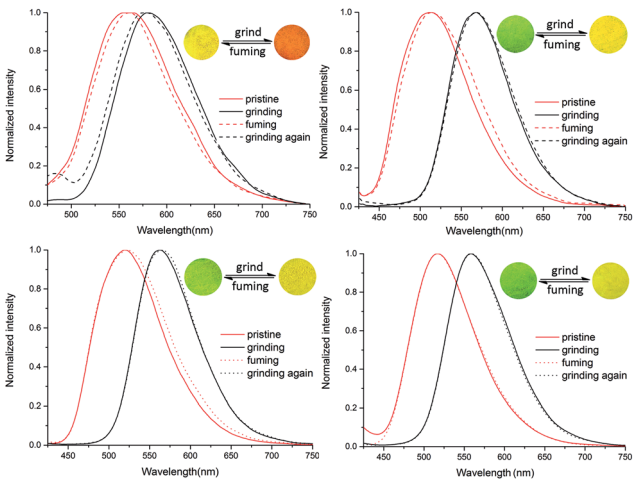

Fig. 4 Normalized fluorescence spectra of (a) **PVBA2**, (b) **PVBA8**, (c) **PVBA12** and (d) **PVBA16** in the solid state under external stimuli. Inset: schematic diagrams of photos under 365 nm light. λ_{ex} = 400 nm.

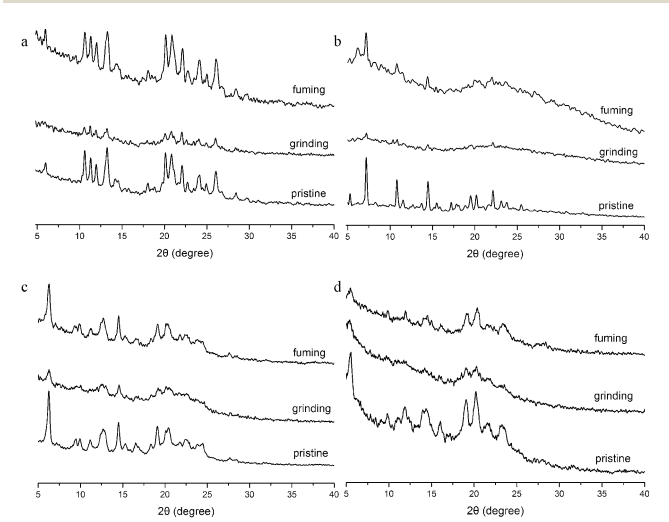

Fig. 5 X-ray powder diffraction of (a) **PVBA2**, (b) **PVBA8**, (c) **PVBA12** and (d) **PVBA16** in the pristine state and after different treatments.

As discussed above, the permeation of solvent vapors into the ground powders increases molecular mobility and then induces color recovery. The increase in temperature also leads to accelerated molecular thermal motion; therefore, the thermal restoration of the ground solids was measured. The result is shown in Fig. 6 and listed in Table S4.† It is clear that the recovery time becomes shorter at higher temperatures and is relative to the length of the alkyl chain at the same temperature. The restoration of the ground compounds with longer alkyl chains needs shorter time at the same temperature.[25] At 110 °C, the ground **PVBA16** powder restored to the original state after 2 s. The recovery time is 3 s for **PVBA12** and 360 s for **PVBA8**, but **PVBA2** cannot be restored even after 2 h. At 50 °C, the fluorescence of the ground **PVBAn** ($n = 2$ and 8) solids was retained for more than one week, but the orange ground **PVBA16** solid converted into a yellow one after 400 s. Another interesting phenomenon is the MFC behavior of the **PVBA16** solid. Note that only the ground **PVBA16** solid emits yellow fluorescence; however, the fluorescence color gradually changed to the original green emission after five days, when it was left standing at room temperature (20 °C). Unlike **PVBA16**, the fluorescence colors and emission spectra of ground **PVBA2**, **PVBA8** and **PVBA12** solids remain for over two weeks at the same temperature. These findings suggest that we can endow bianthracene derivative dyes with stable or self-recovering MFC behavior by tuning the alkyl chain length. MFC materials with tunable recovery behavior could be useful for various applications.

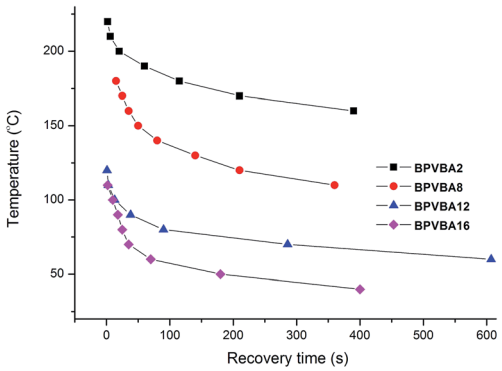

Fig. 6 Plot of recovery time of ground powders *vs.* temperature.

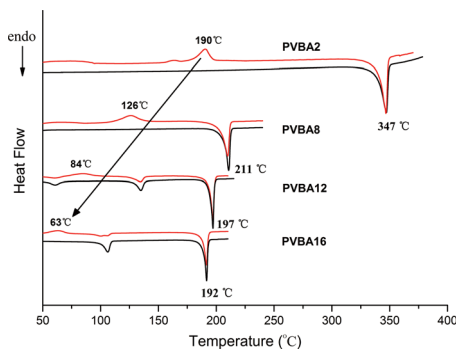

Fig. 7 DSC heat curves of pristine (black) and ground (red) **PVBAn**.

The alkyl length-dependent mechanochromism could be interpreted by DSC experiments. Fig. 7 shows that there is clearly one exothermic transition peak in the lower-temperature region for each ground solid. This broad exothermic peak could be ascribed to the cold-crystallization (crystallizing from glass state) of ground **PVBAn** solids upon annealing[26] and also confirms that the amorphous state is a metastable state. Amorphized **PVBA2**, **PVBA8** and **PVBA12** solids have high exothermic peak values, which result in their stable MFC behaviour at room temperature. The ground **PVBA16** solid could cold-crystallize at room temperature since its exothermic peak is located at 63 °C.[25b,27] Thus, the amorphized **PVBA16** solid induced by grinding rapidly recovered its fluorescence at lower temperatures and even exhibits spontaneous recovering fluorescence properties at room temperature. The reason for the compounds with longer alkyl chain possessing lower phase transition temperatures could be ascribed to the fact that longer alkyl chains provide higher molecular mobility because the ordered packing between alkyl chains becomes disordered more easily relative to aromatic groups with increase in temperature. This point is interpreted by the change in melting points with change in length of the alkyl chain. As shown in Fig. 7, **PVBA2** has the highest melting point at 347 °C, and the lowest melting point at 192 °C is observed for **PVBA16**. In addition, **PVBA12** and **PVBA16** in pristine and ground conditions have an endothermic transition before the melting point, which could be attributed to a crystal phase transition. However, the reason for **PVBA12** and **PVBA16** exhibiting this transition is still unclear, and this phenomenon requires further investigation.

Conclusions

Bowl-shaped phenothiazine and nonplanar bianthracene were integrated into one molecular structure to obtain **PVBAn** ($n = 2$, 8, 12 and 16) with different alkyl chains. The spectral results and quantum chemical calculations indicate that the compounds are D–π–A–π–D molecules. Interestingly, these simple and easily prepared bianthracene derivatives exhibit pronounced and reproducible reversible mechanochromism, which is dependent on the alkyl chain length. XRD and DSC reveal that the transformation between crystalline and amorphous states upon various external stimuli is responsible for the MFC behavior. We have also observed an intriguing MFC behavior of **PVBA16**, as well as an isothermally reversible MFC behavior at room temperature, which is ascribed to the low cold-crystallization temperature. This work has demonstrated that the subtle manipulation of alkyl groups of phenothiazine-based bianthracene could endow these compounds with unique and tunable solid-state optical properties.

Acknowledgements

This work was financially supported by the National Natural Science Foundation of China (21103067, 51403020 and

21374041), the Youth Science Foundation of Jilin Province (20130522134JH), the Open Project of the State Key Laboratory of Supramolecular Structure and Materials (SKLSSM201407), and the Open Project of State Laboratory of Theoretical and Computational Chemistry (K2013-02).

Notes and references

1 (*a*) Y. Sagara and T. Kato, *Nat. Chem.*, 2009, **1**, 605–610; (*b*) Z. Chi, X. Zhang, B. Xu, X. Zhou, C. Ma, Y. Zhang, S. Liu and J. Xu, *Chem. Soc. Rev.*, 2012, **41**, 3878; (*c*) Y. Sagara and T. Kato, *Angew. Chem., Int. Ed.*, 2008, **47**, 5175–5178; (*d*) J. W. Chung, Y. You, H. S. Huh, B. An, S. Yoon, S. H. Kim, S. W. Lee and S. Y. Park, *J. Am. Chem. Soc.*, 2009, **131**, 8163–8172.

2 (*a*) S. S. Babu, V. K. Praveen and A. Ajayaghosh, *Chem. Rev.*, 2014, **114**, 1973–2129; (*b*) A. Seeboth, D. Lötzsch, R. Ruhmann and O. Muehling, *Chem. Rev.*, 2014, **114**, 3037–3068; (*c*) X. Zhu, R. Liu, Y. Li, H. Huang, Q. Wang, D. Wang, X. Zhu, S. Liu and H. Zhu, *Chem. Commun.*, 2014, **50**, 12951–12954; (*d*) J. Andres, R. D. Hersch, J. Moser and A. Chauvin, *Adv. Funct. Mater.*, 2014, **24**, 5029–5036; (*e*) S. Yamane, K. Tanabe, Y. Sagara and T. Kato, *Top. Curr. Chem.*, 2012, **318**, 395–405; (*f*) H. Sun, S. Liu, W. Lin, K. Y. Zhang, W. Lv, X. Huang, F. Huo, H. Yang, G. Jenkins, Q. Zhao and W. Huang, *Nat. Commun.*, 2014, **5**, 3601.

3 N. Zhao, Z. Yang, J. W. Y. Lam, H. H. Y. Sung, N. Xie, S. Chen, H. M. Su, M. Gao, I. D. Williams, K. S. Wong and B. Z. Tang, *Chem. Commun.*, 2012, **48**, 8637–8639.

4 (*a*) M. Aldred, G. Zhang, C. Li, G. Chen, T. Chen and M. Zhu, *J. Mater. Chem. C*, 2013, **1**, 6709; (*b*) A. Pucci and G. Ruggeri, *J. Mater. Chem.*, 2011, **21**, 8282–8291; (*c*) M. M. Caruso, D. A. Davis, Q. Shen, S. A. Odom, N. R. Sottos, S. R. White and J. S. Moore, *Chem. Rev.*, 2009, **109**, 5755–5798; (*d*) K. Ariga, T. Mori and J. P. Hill, *Adv. Mater.*, 2012, **24**, 158–176; (*e*) F. Ciardelli, G. Ruggeri and A. Pucci, *Chem. Soc. Rev.*, 2013, **42**, 857–870.

5 (*a*) Y. Zhang, J. Sun, G. Zhuang, M. Ouyang, Z. Yu, F. Cao, G. Pan, P. Tang, C. Zhang and Y. Ma, *J. Mater. Chem. C*, 2014, **2**, 195; (*b*) Z. Ma, M. Teng, Z. Wang, S. Yang and X. Jia, *Angew. Chem., Int. Ed.*, 2013, **52**, 12268–12272; (*c*) Y. Wang, M. Li, Y. Zhang, J. Yang, S. Zhu, L. Sheng, X. Wang, B. Yang and S. X. Zhang, *Chem. Commun.*, 2013, **49**, 6587–6589; (*d*) C. Ma, B. Xu, G. Xie, J. He, X. Zhou, B. Peng, L. Jiang, B. Xu, W. Tian, Z. Chi, S. Liu, Y. Zhang and J. Xu, *Chem. Commun.*, 2014, **50**, 7374; (*e*) R. Yoshii, A. Nagai, K. Tanaka and Y. Chujo, *Chem.–Eur. J.*, 2013, **19**, 4506–4512; (*f*) M. S. Kwon, J. Gierschner, J. Seo and S. Y. Park, *J. Mater. Chem. C*, 2014, **2**, 2552–2557.

6 (*a*) Y. Sagara, T. Mutai, I. Yoshikawa and K. Araki, *J. Am. Chem. Soc.*, 2007, **129**, 1520–1521; (*b*) S. Yamane, Y. Sagara, T. Mutai, K. Araki and T. Kato, *J. Mater. Chem. C*, 2013, **1**, 2648–2656.

7 Y. Ooyama, G. Ito, H. Fukuoka, T. Nagano, Y. Kagawa, I. Imae, K. Komaguchi and Y. Harima, *Tetrahedron*, 2010, **66**, 7268–7271; Y. Ooyama and Y. Harima, *J. Mater. Chem.*, 2011, **21**, 8372–8380.

8 (*a*) P. Xue, P. Chen, J. Jia, Q. Xu, J. Sun, B. Yao, Z. Zhang and R. Lu, *Chem. Commun.*, 2014, **50**, 2569–2571; (*b*) R. Misra, T. Jadhav, B. Dhokale and S. Mobin, *Chem. Commun.*, 2014, **50**, 9076–9078; (*c*) Y. Gong, Y. Zhang, W. Z. Yuan, J. Z. Sun and Y. Zhang, *J. Phys. Chem. C*, 2014, **118**, 10998–11005; (*d*) X. Zhang, Z. Chi, Y. Zhang, S. Liu and J. Xu, *J. Mater. Chem. C*, 2013, **1**, 3376–3390; (*e*) C. Ma, B. Xu, G. Xie, J. He, X. Zhou, B. Peng, L. Jiang, B. Xu, W. Tian, Z. Chi, S. Liu, Y. Zhang and J. Xu, *Chem. Commun.*, 2014, **50**, 7374–7377; (*f*) X. Cheng, D. Li, Z. Zhang, H. Zhang and Y. Wang, *Org. Lett.*, 2014, **16**, 880–883; (*g*) G. Zhang, J. Lu, M. Sabat and C. L. Fraser, *J. Am. Chem. Soc.*, 2010, **132**, 2160–2162; (*h*) G. Zhang, J. P. Singer, S. E. Kooi, R. E. Evans, E. L. Thomas and C. L. Fraser, *J. Mater. Chem.*, 2011, **21**, 8295–8299; (*i*) R. Yoshii, A. Hirose, K. Tanaka and Y. Chujo, *Chem.–Eur. J.*, 2014, **20**, 8320–8324.

9 (*a*) J. Jia, K. Cao, P. Xue, Y. Zhang, H. Zhou and R. Lu, *Tetrahedron*, 2012, **68**, 3626–3632; (*b*) X. Yang, R. Lu, P. Xue, B. Li, D. Xu, T. Xu and Y. Zhao, *Langmuir*, 2008, **24**, 13730–13735; (*c*) Y. Gong, Y. Zhang, W. Yuan, J. Sun and Y. Zhang, *J. Phys. Chem. C*, 2014, **118**, 10998–11005.

10 (*a*) P. Xue, B. Yao, J. Sun, Q. Xu, P. Chen, Z. Zhang and R. Lu, *J. Mater. Chem. C*, 2014, **2**, 3942–3950; (*b*) X. Zhang, Z. Chi, J. Zhang, H. Li, B. Xu, X. Li, S. Liu, Y. Zhang and J. Xu, *J. Phys. Chem. B*, 2011, **115**, 7606–7611.

11 (*a*) P. Zhang, W. Dou, Z. Ju, L. Yang, X. Tang, W. Liu and Y. Wu, *Org. Electron.*, 2013, **14**, 915–925; (*b*) M. Sarkar and A. Saman, *Acta Crystallogr., Sect. E: Struct. Rep. Online*, 2003, **59**, o1764.

12 Y. Han, H. Cao, H. Sun, Y. Wu, G. Shan, Z. Su, X. Hou and Y. Liao, *J. Mater. Chem. C*, 2014, **2**, 7648–7655; L. Bu, M. Sun, D. Zhang, W. Liu, Y. Wang, M. Zheng, S. Xue and W. Yang, *J. Mater. Chem. C*, 2013, **1**, 2028–2035.

13 (*a*) P. Natarajan and M. Schmittel, *J. Org. Chem.*, 2013, **78**, 10383–10394; (*b*) Y. Yu, Z. Wu, Z. Li, B. Jiao, L. Li, L. Ma, D. Wang, G. Zhou and X. Hou, *J. Mater. Chem. C*, 2013, **1**, 8117; (*c*) L. Kong, J. Yang, Z. Xue, H. Zhou, L. Cheng, Q. Zhang, J. Wu, B. Jin, S. Zhang and Y. Tian, *J. Mater. Chem. C*, 2013, **1**, 5047–5505; (*d*) Z. Iqbal, W. Wu, H. Zhang, P. Hua, X. Fang, D. Kuang, L. Wang, H. Meier and D. Cao, *Dyes Pigm.*, 2013, **99**, 299–307.

14 (*a*) Z. Guo, Z. Jin, J. Wang and J. Pei, *Chem. Commun.*, 2014, **50**, 6088; (*b*) Y. Gong, Y. Tan, J. Liu, P. Lu, C. Feng, W. Yuan, Y. Lu, J. Sun, G. He and Y. Zhang, *Chem. Commun.*, 2013, **49**, 4009–4011; (*c*) Y. Sagra and T. Kato, *Angew. Chem., Int. Ed.*, 2011, **50**, 9128–9132.

15 (*a*) X. Liu, X. Zhang, R. Lu, P. Xue, D. Xu and H. Zhou, *J. Mater. Chem.*, 2011, **21**, 8756; (*b*) X. Liu, D. Xu, R. Lu, B. Li, C. Qian, P. Xue, X. Zhang and H. Zhou, *Chem.–Eur. J.*, 2011, **17**, 1660–1669; (*c*) P. Xue, Q. Xu, P. Gong, C. Qian, Z. Zhang, J. Jia, X. Zhao, R. Lu, A. Ren and T. Zhang, *RSC Adv.*, 2013, **3**, 26403–26411; (*d*) C. Zhao, A. Wakamiya, Y. Inukai and S. Yamaguchi, *J. Am. Chem. Soc.*, 2006, **128**, 15934–15935.

16 J. S. Yang, K. L. Liau, C. M. Wang and C. Y. Hwang, *J. Am. Chem. Soc.*, 2004, **126**, 12325–12335.

17 (*a*) J. Sun, X. Lv, P. Wang, Y. Zhang, Y. Dai, Q. Wu, M. Ouyang and C. Zhang, *J. Mater. Chem. C*, 2014, **2**, 5365; (*b*) L. Bu, M. Sun, D. Zhang, W. Liu, Y. Wang, M. Zheng, S. Xue and W. Yang, *J. Mater. Chem. C*, 2013, **1**, 2028.

18 (*a*) P. Xue, R. Lu, G. Chen, Y. Zhang, H. Nomoto, M. Takafuji and H. Ihara, *Chem.–Eur. J.*, 2007, **13**, 8231–8239; (*b*) M. Yang, D. Xu, W. Xi, L. Wang, J. Zheng, J. Huang, J. Zhang, H. Zhou, J. Xu and Y. Tian, *J. Org. Chem.*, 2013, **78**, 10344–10359.

19 T. R. Zhang, R. Lu, H. Y. Zhang, P. C. Xue, W. Feng, X. L. Liu, B. Zhao, Y. Y. Zhao, T. J. Li and J. N. Yao, *J. Mater. Chem.*, 2003, **13**, 580–584.

20 (*a*) X. Sun, X. Zhang, X. Li, S. Liu and G. Zhang, *J. Mater. Chem.*, 2012, **22**, 17332–17339; (*b*) C. Vijayakumar, V. K. Praveen, K. K. Kartha and A. Ajayaghosh, *Phys. Chem. Chem. Phys.*, 2011, **13**, 4942–4949; (*c*) P. Xue, R. Lu, P. Zhang, J. Jia, Q. Xu, T. Zhang, M. Takafuji and H. Ihara, *Langmuir*, 2013, **29**, 417–425.

21 S. Yamane, Y. Sagara, T. Mutai, K. Araki and T. Kato, *J. Mater. Chem. C*, 2013, **1**, 2648–2656.

22 (*a*) X. Shen, Y. Wang, E. Zhao, W. Yuan, Y. Liu, P. Lu, A. Qin, Y. Ma, J. Sun and B. Tang, *J. Phys. Chem. C*, 2013, **117**, 7334–7347; (*b*) K. Kawaguchi, T. Seki, T. Karatsu, A. Kitamura, H. Ito and S. Yagai, *Chem. Commun.*, 2013, **49**, 11391–11393; (*c*) Y. Wang, W. Liu, L. Bu, J. Li, M. Zheng, D. Zhang, M. Sun, Y. Tao, S. Xue and W. Yang, *J. Mater. Chem. C*, 2013, **1**, 856–862; (*d*) W. Liu, Y. Wang, M. Sun, D. Zhang, M. Zheng and W. Yang, *Chem. Commun.*, 2013, **49**, 6042–6044.

23 (*a*) B. Zhang, C. Hsu, Z. Yu, S. Yang and E. Chen, *Chem. Commun.*, 2013, **49**, 8872–8874; (*b*) T. Wen, D. Zhang, J. Liu, R. Lin and J. Zhang, *Chem. Commun.*, 2013, **49**, 5660–5662.

24 J. Wang, J. Mei, R. Hu, J. Z. Sun, A. Qin and B. Z. Tang, *J. Am. Chem. Soc.*, 2012, **134**, 9956–9966.

25 (*a*) N. D. Nguyen, G. Zhang, J. Lu, A. E. Sherman and C. L. Fraser, *J. Mater. Chem.*, 2011, **21**, 8409–8415; (*b*) M. Zheng, D. T. Zhang, M. X. Sun, Y. P. Li, T. L. Liu, S. F. Xue and W. J. Yang, *J. Mater. Chem. C*, 2014, **2**, 1913–1920.

26 (*a*) N. Vasanthan, N. Jyothi Manne and A. Krishnama, *Ind. Eng. Chem. Res.*, 2013, **52**, 17920–17926; (*b*) P. Supaphol and J. E. Spruiell, *Polymer*, 2001, **42**, 699–712.

27 (*a*) N. Mizoshita, T. Tani and S. Inagaki, *Adv. Mater.*, 2012, **24**, 3350–3355; (*b*) X. Luo, J. Li, C. Li, L. Heng, Y. Q. Dong, Z. Liu, Z. Bo and B. Z. Tang, *Adv. Mater.*, 2011, **23**, 3261–3265.

